12-1-2017

Treatment with AICAR inhibits blastocyst development, trophectodermdifferentiation and tight junction formation and function in mice

Michele D. Calder
Western University

Nicole A. Edwards
Western University

Dean H. Betts
Western University, dean.betts@schulich.uwo.ca

Andrew J. Watson
Western University

Molecular Human Reproduction, Vol.23, No.11 pp. 771–785, 2017
Advanced Access publication on September 28, 2017 doi:10.1093/molehr/gax050

molecular human reproduction

ORIGINAL ARTICLE

Treatment with AICAR inhibits blastocyst development, trophectoderm differentiation and tight junction formation and function in mice

Michele D. Calder[1,2,*], Nicole A. Edwards[1], Dean H. Betts[1,2,3], and Andrew J. Watson[1,2,3]

[1]Departments of Physiology and Pharmacology, Western University, London, Ontario, Canada [2]Obstetrics and Gynaecology, Schulich School of Medicine, Western University, London, Ontario, Canada [3]Children's Health Research Institute (CHRI), Lawson Health Research Institute (LHRI), London, Ontario, Canada

*Correspondence address. Dental Sciences Rm. 00066; Medical Science Building, 1151 Richmond St. N, London, Ontario, Canada. Tel: +1-519-661-2111x86925; Fax: +1-519-661-3827; E-mail: Michele.Calder@schulich.uwo.ca

Submitted on October 7, 2016; resubmitted on August 18, 2017; editorial decision on August 30, 2017; accepted on September 6, 2017

STUDY QUESTION: What is the impact of adenosine monophosphate-activated protein kinase (AMPK) activation on blastocyst formation, gene expression, and tight junction formation and function?

SUMMARY ANSWER: AMPK activity must be tightly controlled for normal preimplantation development and blastocyst formation to occur.

WHAT IS KNOWN ALREADY: AMPK isoforms are detectable in oocytes, cumulus cells and preimplantation embryos. Cultured embryos are subject to many stresses that can activate AMPK.

STUDY DESIGN, SIZE, DURATION: Two primary experiments were carried out to determine the effect of AICAR treatment on embryo development and maintenance of the blastocoel cavity. Embryos were recovered from superovulated mice. First, 2-cell embryos were treated with a concentration series (0–2000 μM) of AICAR for 48 h until blastocyst formation would normally occur. In the second experiment, expanded mouse blastocysts were treated for 9 h with 1000 μM AICAR.

PARTICIPANTS/MATERIALS, SETTING, METHODS: Outcomes measured included development to the blastocyst stage, cell number, blastocyst volume, AMPK phosphorylation, *Cdx2* and blastocyst formation gene family expression (mRNAs and protein measured using quantitative RT-PCR, immunoblotting, immunofluorescence), tight junction function (FITC dextran dye uptake assay), and blastocyst ATP levels. The reversibility of AICAR treatment was assessed using Compound C (CC), a well-known inhibitor of AMPK, alone or in combination with AICAR.

MAIN RESULTS AND THE ROLE OF CHANCE: Prolonged treatment with AICAR from the 2-cell stage onward decreases blastocyst formation, reduces total cell number, embryo diameter, leads to loss of trophectoderm cell contacts and membrane zona occludens-1 staining, and increased nuclear condensation. Treatment with CC alone inhibited blastocyst development only at concentrations that are higher than normally used. AICAR treated embryos displayed altered mRNA and protein levels of blastocyst formation genes. Treatment of blastocysts with AICAR for 9 h induced blastocyst collapse, altered blastocyst formation gene expression, increased tight junction permeability and decreased CDX2. Treated blastocysts displayed three phenotypes: those that were unaffected by treatment, those in which treatment was reversible, and those in which effects were irreversible.

LARGE SCALE DATA: Not applicable.

LIMITATIONS, REASONS FOR CAUTION: Our study investigates the effects of AICAR treatment on early development. While AICAR does increase AMPK activity and this is demonstrated in our study, AICAR is not a natural regulator of AMPK activity and some

outcomes may result from off target non-AMPK AICAR regulated events. To support our results, blastocyst developmental outcomes were confirmed with two other well-known small molecule activators of AMPK, metformin and phenformin.

WIDER IMPLICATIONS OF THE FINDINGS: Metformin, an AMPK activator, is widely used to treat type II diabetes and polycystic ovarian disorder (PCOS). Our results indicate that early embryonic AMPK levels must be tightly regulated to ensure normal preimplantation development. Thus, use of metformin should be carefully considered during preimplantation and early post-embryo transfer phases of fertility treatment cycles.

STUDY FUNDING AND COMPETING INTEREST(S): Canadian Institutes of Health Research (CIHR) operating funds. There are no competing interests.

Key words: AMPK / stress pathways / embryo culture / assisted reproductive technologies / preimplantation / blastocyst formation

Introduction

In mammals, preimplantation development begins at fertilization and ends with the formation of the fluid-filled blastocyst, which hatches from the zona pellucida and implants in the uterine wall to establish a pregnancy (MacPhee *et al.*, 2000; Watson *et al.*, 2004). The early blastocyst consists of two cell types: the inner cell mass (ICM) and the trophectoderm (TE) (Watson *et al.*, 2004). The ICM at this stage is composed of undifferentiated cells that later will become the embryo proper. The TE mediates implantation into the uterus and becomes the embryonic part of the placenta. The TE is characterized by the expression of early transcription factors such as caudal homeobox two (CDX2, Strumpf *et al.*, 2005). Tight junctions (TJ), containing zona occludens-1 (ZO-1, TJP1) and occludin (OCLN), form a seal between TE cells, which is critical for fluid accumulation within the blastocyst cavity (Fleming *et al.*, 1989; Kim *et al.*, 2004; Violette *et al.*, 2006; Bell and Watson, 2013). The activity of the Na+/K+ ATPase establishes an ionic gradient that drives fluid accumulation in the cavity, and regulates TE tight junction development and function (Betts *et al.*, 1998; Violette *et al.*, 2006; Madan *et al.*, 2007). ATPase Na+/K+ transporting subunit beta 1 (*Atp1b1*) knockdowns are embryonic lethal, as embryos arrest at the morula stage (Madan *et al.*, 2007). In addition, aquaporins (AQP) are localized to the TE membrane and facilitate water movement into the blastocyst cavity (Barcroft *et al.*, 2003). Other important genes that may measure preimplantation embryo developmental competence are those involved with embryonic arrest. Growth arrest DNA damage-inducible alpha (GADD45A) is involved in cell cycle arrest when there is DNA damage, to give time to repair the damage (reviewed in Zhan, 2005).

A gene critical for the embryonic response to environmental changes is adenosine monophosphate-activated protein kinase (AMPK). AMPK is a master regulator of cellular glucose and lipid metabolism (reviewed in Hardie *et al.*, 2012). Phosphorylation of AMPK activates catabolic pathways to generate ATP (i.e. fatty acid oxidation and glycolysis) and shuts down anabolic pathways to conserve energy (i.e. lipo-, sterol- and gluconeogenesis) (Corton *et al.*, 1995; Zhou *et al.*, 2001; Hardie, 2011; Hardie *et al.*, 2012). The signaling cascades can result in phosphorylation of acetyl CoA carboxylase (ACC), which would inactivate lipid synthesis (Carling *et al.*, 1989), and therefore phosphorylated ACC is commonly used as a marker of AMPK activation (Zhou *et al.*, 2001). AMPK is activated when the ratio of AMP/ATP changes, or as a result of hormones, hypo- or hyperglycemia, hyperosmolarity, exercise and oxidative stress (Hardie *et al.*, 2012). AMPK phosphorylation and activity can be decreased in cultured cells by exposure to high glucose concentrations (da Silva Xavier *et al.*, 2000) and is decreased in diabetes and obesity (Liu *et al.*, 2006; Blume *et al.*, 2007). Metformin is a commonly used oral diabetes drug which increases activation of AMPK (Zhou *et al.*, 2001). Metformin is widely used in infertile women to treat insulin resistance due to polycystic ovarian syndrome (PCOS), to restore spontaneous ovulatory cycles (Nestler *et al.*, 1998), or to improve response to other ART therapies (Nestler *et al.*, 1998; Tang *et al.*, 2006; Palomba *et al.*, 2014). In cultured cells, AICAR (5-aminoimidazole-4-carboxamide ribonucleotide) is often used to activate AMPK as it is metabolized to an AMP mimetic, resulting in unchanged ATP levels (Corton *et al.*, 1995; Zhou *et al.*, 2001) Frequently used experimental concentrations of AICAR range from 0.5 to 2 mM (Chen *et al.*, 2006; Guo *et al.*, 2009). AICAR and metformin have similar effects on AMPK and targets (Zhou *et al.*, 2001; Blume *et al.*, 2007). Compound C (CC) is an AMPK inhibitor that competes for binding with ATP (Zhou *et al.*, 2001) and is typically used at concentrations between 5 and 20 μM (Zhou *et al.*, 2001; Chen *et al.*, 2006; Xie *et al.*, 2013). In addition, AICAR and metformin have AMPK-independent effects (Guo *et al.*, 2009; Liu *et al.*, 2014). One of these effects may be the regulation of the mTOR pathway, resulting in the reduced phosphorylation of ribosomal protein S6 (Guo *et al.*, 2009; Klubo-Gwiezdzinska *et al.*, 2012).

AMPK is composed of a heterotrimer of α, β and γ subunits (reviewed in Hardie, 2011). The catalytic subunits of AMPK (α1 and α2, PRKAA1 and PRKAA2) are encoded by separate genes and both proteins are detectable in oocytes and cumulus cells (Downs *et al.*, 2002). β and γ subunit mRNAs are also expressed in cumulus and oocytes (Mayes *et al.*, 2007). Activation of AMPK improves meiosis of mouse oocytes cultured under inhibitory conditions (Downs *et al.*, 2002). However, activation of AMPK with either AICAR or metformin has the opposite effect in bovine and porcine cumulus-oocyte complexes and delays maturation (Mayes *et al.*, 2007; Tosca *et al.*, 2007; Bilodeau-Goeseels *et al.*, 2011, 2014). Knockout of individual PRKA isoforms in mice does not seem to produce reproductive phenotypes *in vivo*. However, oocyte-specific protein kinase AMP-activated catalytic subunit alpha 1 (*Prkaa1*) knockout reduced *in vitro* mouse embryo development (Bertoldo *et al.*, 2015), and this may be due to higher stress imposed on cultured embryos. Embryos cultured *in vitro* are exposed to many stresses such as hyperosmolarity, variations in temperature, pH, oxygen, metabolic substrate concentrations, light exposure and pipetting (Xie *et al.*, 2007; Wale and Gardner, 2016). Stresses such as hyperosmolarity can activate AMPK in embryos, embryonic stem cells, and trophoblast stem cells, and can induce the differentiation of trophoblast stem cells (Zhong *et al.*, 2010). Activators of

AMPK, AICAR (1 mM) and metformin (25 μg/ml, 151 μM), improved development of mouse embryos cultured in inhibitory conditions (Eng *et al.*, 2007). AICAR (250 μM) improved meiotic competence in oocytes of diabetic mice in which AMPK activity is decreased (Ratchford *et al.*, 2007). Metformin (25 μg/ml) treatment increased phosphorylation of AMPK and reduced apoptosis in blastocysts of obese mice (Louden *et al.*, 2014). In contrast, exposure to 10 μM metformin caused early bovine embryos to arrest (Pikiou *et al.*, 2013). In summary, experimental evidence suggests that AMPK activity must be regulated within narrow limits to achieve optimal preimplantation embryo development.

The purpose of our study was to characterize the impact of AICAR treatment and thus AMPK activation on preimplantation development in the mouse. We investigated effects on development and to protein and mRNA levels of several blastocyst formation gene families and markers of embryonic developmental competence. We also assessed the effects of AMPK activation on TE tight junction function and permeability. Prolonged AICAR treatment leads to loss of cell-to-cell contacts, loss of membrane ZO-1 staining, and nuclear condensation. Embryos treated with AICAR had decreased transcript levels of several blastocyst formation gene family members. Blastocysts treated with AICAR for only 9 h begin to collapse and in many, this developmental defect was irreversible. These results establish a foundation for investigating the roles of AMPK during early development and its contribution to regulating early embryo developmental competence and blastocyst formation. These outcomes are especially important due to the increased use of metformin to treat PCOS in humans, as systemic metformin may impact AMPK activity and blastocyst formation in early embryos from treated women.

Materials and Methods

Mouse embryos collection and culture

Three to four-week-old female CD-1 mice and adult male CD-1 mice (4–8 months) were obtained from Charles River, Canada. Females were injected with 7.5 IU pregnant mare serum gonadotrophin (PMSG; Folligon, Intervet, Whitby, ON) to stimulate follicular development, followed by 7.5 IU human chorionic gonadotrophin (hCG; Chorulon, Intervet) 46–48 h after PMSG and placed with a male for mating. Female mice were assessed for the presence of a vaginal plug. If one was present, the embryonic age was classified as E0.5 (Edwards *et al.*, 2016). Two-cell embryos were flushed from oviducts with M2 (Sigma, Oakville, ON) 46–48 h post hCG injection, washed, and placed into culture in KSOM (KSOMaa Evolve®, Zenith Biotech, Guilford, CT, USA) at 37°C in a 5% O_2, 5% CO_2 and 90% N_2 atmosphere (Edwards *et al.*, 2016).

Ethical approval

Animal care and handling was according to the guidelines of the Western University Animal Care Committee approved by the Canadian Council on Animal Care (Protocol number Watson 2010-021).

Effects of AMPK activator (AICAR) on embryo development, diameter and cell count

Mice were superovulated as described above. Two-cell embryos were cultured to the blastocyst stage and collected at 96 h post hCG injection. Initially, embryos were cultured between concentrations of 0–2000 μM of AICAR (Sigma) diluted from a 25 mM stock solution in KSOM. Embryos were evaluated for development to the blastocyst stage at 96 h after hCG (48 h culture from 2-cell). Further experiments were carried out with the selected optimal dose of 1000 μM AICAR. Photomicrographs were taken using a Leica microscope for measurement of embryo diameter. Embryos were then either fixed using 2% paraformaldehyde and stored until later use for confocal microscopy or frozen at −80°C for later RNA analysis. To determine total cell number DAPI-stained nuclei were counted on every 5 μM as z-stacks through each embryo. Two other known AMPK activators, metformin 0–1000 μM and phenformin 0–25 μM were tested to investigate the consistency of outcomes.

Dose response experiments with the AMPK inhibitor Compound C (CC, P5499, Sigma) were done in MF-1 mice (Harlan, Indianapolis, IN) in EmbryoMax KSOM medium from EMD Millipore (Billerica, MA) in 2-cell embryos treated for 48 h. CC was stored as a 10 mM stock solution in DMSO. Later experiments used a dosage of 10 and 20 μM CC only or in combination with 1000 μM AICAR (embryos were pretreated with CC only for 3 h) in our standard culture conditions with CD-1 mice. Two cell embryos were cultured for 48 h and examined for blastocyst development and stored in radioimmunoprecipitation assay buffer (RIPA, 150 mM NaCl, 1% Triton X-100, 0.5% sodium deoxycholate, 0.1% SDS, 50 mM Tris) for Western blot experiments as detailed below.

Whole-mount immunofluorescent confocal microscopy

For immunofluorescent microscopy, embryos were fixed in 2% paraformaldehyde in phosphate buffered saline (PBS) for 20 min at room temperature and stored in PHEM (60 mM PIPES, 25 mM HEPES, 10 mM EGTA, 1 mM $MgCl_2$-6 H_2O) buffer at 4°C. For immunostaining, fixed embryos were permeabilized and blocked in 5% donkey serum (Cedarlane, Burlington, ON) + 0.01% Triton X-100 in PBS for 1 h at room temperature (Madan *et al.*, 2007). All other steps were performed in antibody dilution buffer (0.5% donkey serum + 0.005% Triton X-100) in PBS. Embryos were then incubated overnight at 4°C in the following primary antibodies at the indicated dilutions: rabbit anti-CDX2 (ab76541, 1:100, Abcam, Cambridge, MA, USA), rabbit anti-phospho-AMPK (07–681, 1:75, Millipore, Temecula, CA), rat anti-ZO1 (MABT11, 1:100, Millipore, Temecula, CA), rat anti-AQP9 (AQP91-A, 1:100, Alpha Diagnostic International, San Antonio, TX), mouse anti-CDH1 (C20820, 1:100, BD Transduction Laboratories, San Jose CA). Embryos were then incubated in the following secondary antibodies at a 1:200 dilution: donkey anti-rabbit (711-095-152), donkey anti-rat (712-095-153) or donkey anti-mouse (715-095-151, CDH1) conjugated to FITC (Jackson ImmunoResearch, West Grove, PA, USA). Embryos were counterstained with rhodamine-phalloidin to stain filamentous actin and DAPI to stain DNA (Sigma Aldrich, Canada) (Madan *et al.*, 2007). Negative control embryos were not exposed to primary antibody. Embryos were examined by laser-scanning confocal microscopy (Olympus FV1000, Olympus Canada Inc., Markham, ON). Z-stack slices were taken every 5 μM through each embryo to count blue DAPI-stained cell nuclei.

RNA isolation, reverse transcription and real-time PCR

Total RNA was extracted from similarly sized pools of frozen embryos using a Picopure kit according to manufacturer's instructions (Arcturus, Mountain View, CA, USA). Samples were spiked with exogenous control Luciferase mRNA (Promega Corporation, Madison, WI, USA) at 0.025 pg/embryo prior to extraction (Fong *et al.*, 2007). Removal of genomic DNA was performed with a DNAse I digestion step (Qiagen, Mississauga, ON). Following extraction, the eluted volume was 11 μl. RNA

samples were reverse transcribed (RT) with Sensicript (Qiagen) in a mix containing 2 µl 10× buffer, 1 µl 10 mM dNTPs, 2 µl 10 µM anchored oligodT_{23} (1 µM final concentration, Sigma) and 1 µl 10 µM random nonamers (0.5 µM final concentration, Sigma), 1 µl 10 U/µl RNAse inhibitor (Life Technologies, Burlington, ON) and 1 µl Sensiscript in a volume of 20 µl. The reaction was carried out for 10 min at 25°C, followed by 90 min at 37°C in a thermocycler.

For real-time qPCR, we used the external (Luciferase) control for quantification (Fong *et al.*, 2007). PCR was performed in a Bio-Rad CFX384 Real-time system (Bio-Rad, Mississauga, ON) using TaqMan® Gene Expression Assays (Applied Biosystems, Foster City, CA, USA). A custom Taqman® primer and probe set for Luciferase were designed using the Applied Biosystems Assays-by-Design File Builder program (Fong *et al.*, 2007). Commercially available TaqMan® Gene Expression Assays for *Cdx2* (caudal homeobox domain 2, Mm01212880_m1), *Cdh1* (E-cadherin, Mm00486918_m1), *Aqp9* (aquaporin 9, Mm00508094_m1), *Ocln* (occludin, Mm00500912_m1), *Tjp1* (tight junction protein 1, ZO1, Mm00493699_m1), *Actb* (beta actin, Mm01205647_g1), *Gadd45a* (growth arrest and DNA damage-inducible 45 alpha, Mm00432802_m1), *Atp1b1* (Na+/K+ ATPase β1 subunit, Mm00437612_m1) and *Atp1a1* (Na+/K+ ATPase α1 subunit, Mm00523255_m1) were used to assess effects to mRNA transcript relative levels. Standard cycling conditions were 50° for 2 min, 95° for 5 min, followed by 50 cycles of 95° for 15 s and 60° for 1 min.

Western blots

Western blots were carried out according to protocols developed by Edwards *et al.* (2016). Thirty control or 1000 µM AICAR treated embryos after 48 h of culture from the two cell stage were stored in RIPA buffer at −80°C until use. Total protein lysates were resolved on a 4–12% Bis-Tris gel (Life Technologies) and transferred to a polyvinylidene difluoride (PVDF) membrane. Membranes were cut into three pieces, above 100 kDa, 50–100 kDa and below 50 kDa. Membranes were blocked in 5% skimmed milk or 5% bovine serum albumin in Tris-buffered saline-Tween 20 (TBS-T) for 1 h at room temperature, followed by overnight incubation in primary antibody at 4°C. Membranes were then incubated in secondary antibody goat anti-rabbit-horseradish peroxidase (HRP) (Cell Signaling 7074, Danvers, MA) for 1 h at room temperature. A mouse monoclonal antibody against β-actin conjugated to HRP (A3854, Sigma, 1:20 000), was used as a protein loading control. Membranes were visualized by detection of Forte ECL (EMD Millipore, Billerica, MA). Densitometry analysis was performed in Image Lab 4.0 (Bio-Rad). Primary antibodies used: anti-CDX2 (Abcam, Cambridge, MA, ab76541,1:500), anti-phospho-AMPKα (Thr172) (EMD Millipore 07–681, 1:500), anti-AMPKα (Cell Signaling 5831, 1:500), anti-phospho-ACC (ser79, Cell Signaling 3661, 1:250), anti-ACC (Cell Signaling 3676, 1:1000) anti-E-cadherin (BD Transduction Laboratories C20820, 1:500). Phospho-ribosomal protein S6 (ser235/236, Cell Signaling 4858) was detected as part of the PathScan multiple protein cocktail (CS 5301).

Embryo recovery from AICAR treatment: embryo development, diameter and cell counts

Mice were superovulated as described above. Two-cell embryos were flushed from oviducts with M2 on E1.5, washed with KSOMaa, and placed into culture at 37°C in 5% CO_2, 5% O_2 and 90% N_2 atmosphere for 48 h. Embryos that had formed blastocysts were separated, washed and placed into culture with either 0 or 1000 µM AICAR for 9 h. Blastocyst morphology and cavity volume were assessed and recorded on photomicrographs taken with a Leica microscope. Embryos were then washed in KSOMaa Evolve. AICAR-treated embryos were separated into those that: (1) remained a blastocyst or (2) those that collapsed (i.e. 75% or greater reduction in blastocyst cavity) for an additional 24 h in drug free culture medium to assess recovery rates. The percentage of blastocysts with fully expanded blastocyst cavities at 24 h of recovery time was measured. Photomicrographs were again taken for measurement of embryo diameter. Embryos were then fixed or frozen for real-time PCR studies as described above.

Quantification of CDX2 and F-actin staining

Embryos were stained and mounted on slides as described above. Microscopic images were obtained using a confocal microscope (Olympus) at a magnification of 40×, converted to tiff files and fluorescence intensity was measured using ImageJ software (National Institutes of Health, Bethesda, MD, USA). The oval tool was used to draw a record of interest (ROI) around the blastocyst. For CDX2, background was calculated from the mean of ROI of the negative controls (no primary antibody) and was subtracted from the ROI of the control and AICAR treated embryos. F-actin was not adjusted for background, as all groups had actin staining.

Measurement of tight junction permeability by FITC-dextran uptake assay

Embryos were cultured from the two-cell stage to blastocysts in KSOM Evolve. Blastocysts were sorted into control and 1000 µM AICAR groups and incubated for 9 h. For a positive control, blastocysts were placed into culture with KSOM containing 2 mM EGTA (ethylene glycol Bis-(β-aminoethyl ether) *N,N,N,N* tetraacetic acid) for 30 min to disrupt adherens junctions (Violette *et al.*, 2006; Bell and Watson, 2013). After incubation all treatment groups were placed into 20 µl drops of KSOM containing 1 mg/ml 40 kDa FITC-Dextran (Sigma) for 30 min. Following this, blastocysts from each group were washed separately three times in 50 µl wash drops of KSOM and placed into a final fresh KSOM drop for immediate morphological assessment using a Leica compound fluorescent microscope equipped with a camera.

ATP assay

A Luminescent ATP Detection Assay kit (ab113849, Abcam) was used to measure total blastocyst ATP with the following modifications made from the manufacturer's protocol according to Edwards *et al.* (2016). ATP standards between 0.78125 pM and 100 pM were diluted in water and added in a volume of 10–100 µl KSOM. Five control and 48 h AICAR-treated embryos were placed into a volume of 100 µl KSOM in wells of a 96-well plate. Wells containing KSOM only were blank controls. Luminescence read on a Spectromax M5 plate reader (Molecular Devices, Sunnyvale, CA) at 450 nm. A standard curve was generated with the luminescence detected minus the average of the blank controls. Control or AICAR samples minus blanks were calculated from the standard curve. Data were analyzed using SoftMax Pro software (Molecular Devices).

Statistical analysis

A one-way ANOVA was performed for developmental frequencies (%) of two-cell embryos treated with various doses of AICAR, CC, metformin or phenformin. A Holm-Sidak test was used to test for differences among means. *T*-tests were used to test for differences in diameters and cell numbers between control and 1000 µM AICAR-treated embryos, as well as ATP concentrations. A Mann–Whitney *U* statistic was used to determine differences between blastocysts that were not treated or treated with AICAR for 9 h. The data was not normally distributed because all control embryos remained at the blastocyst stage while some AICAR-treated

embryos collapsed. The data is reported as the median percentage. When we examined embryos after 24 h recovery, a non-parametric Rank ANOVA was used due to unequal variation since controls remained all blastocysts. A Tukey test was used for multiple comparisons. For qRT-PCR samples, quantification was normalized to the exogenous control luciferase RNA levels. Expression levels were calculated according to the method of Pfaffl (2001), where expression level is calculated as the ratio between $Etarget^{\Delta CT(target\ gene)}/ELuc^{\Delta CT(Luc)}$. E = Efficiency of the primer set, which was calculated by the slope of 10-fold dilutions of a standard sample according to the formula of $E = 10^{(-1/slope)}$. The ΔC_T value = C_T(avg of control) – C_T(each sample). Statistical analysis was performed using SigmaStat® 3.5 (Jandel Scientific Software, San Rafael, CA, USA) software package. Real-time qRT-PCR results are presented as the mean ± standard error of the mean (SEM).

Results

AICAR treatment caused an inhibition of preimplantation development

AICAR treatment caused a dose-dependent inhibition in embryo development. Significantly fewer two-cell embryos developed to the blastocyst stage after 48 h of culture at a concentration of 500, 1000 and 2000 μM AICAR (45.9, 26.6 and 9.4% blastocyst development, respectively, Fig. 1A). Development of 0, 10 and 100 μM AICAR-treated embryos did not vary significantly from one another and resulted in blastocyst developmental frequencies of 65–80%. Thus, the 1000 μM dose of AICAR was selected as an optimal dose for all further experiments. Blastocyst total cell number was significantly lower after 48 h of 1000 μM AICAR treatment (Fig. 1B). Most AICAR-treated embryos arrested at the morula stage. Additionally, embryo diameter was significantly reduced after 48 h AICAR treatment (Fig. 1C). Two other known AMPK activators, metformin (Supplementary Fig. S1A) and phenformin (Supplementary Fig. S1B) displayed significant dose-dependent negative effects on embryo development as well.

We also investigated the effects of treatment with a commonly used inhibitor of the AMPK pathway, Compound C (CC). In our hands, embryo development was not detectably inhibited until higher (100 μM, Supplementary Fig. S1C) than normally used concentrations (10 μM), but even this decrease was not statistically significant. The 100 μM dose however did have a significant effect on embryo diameter (data not shown). When treated with 10 and 20 μM CC, embryo development was not affected and the effects of AICAR were not reversed when treated in combination (Supplementary Fig. S1D).

AICAR treatment increased phosphorylated AMPK and decreased blastocyst formation proteins

AICAR potently stimulated the fluorescence intensity of phosphorylated AMPK (p-AMPK; Fig. 2A). Embryos treated with AICAR for 48 h displayed a staining pattern of zona occludens-1 (ZO-1, TJP1) that varied dramatically from that of control embryos. In controls, ZO1 was present at cell borders and co-localized with actin (yellow staining in merged channel, Fig. 2B) while ZO1 was predominantly cytoplasmic in AICAR-treated embryos. AQP9 fluorescence intensity was also decreased at the cell membranes in AICAR-treated embryos (Fig. 3A). In contrast, no obvious effect to E-cadherin (E-cad, CDH1) staining was observed (Fig. 3B). E-cadherin maintained its normal localization to surrounding cell borders in AICAR-treated embryos (Fig. 3B). F-Actin (red staining) however, was often decreased after AICAR treatment (Figs. 2A, B and 3 A, B). Some embryos displayed cell rounding and apparent loss of cell-to-cell contacts (arrowheads, Fig. 2A). In addition, some AICAR-treated embryos showed signs of nuclear condensation, (arrows, Fig. 2A), which is a common early sign of apoptosis.

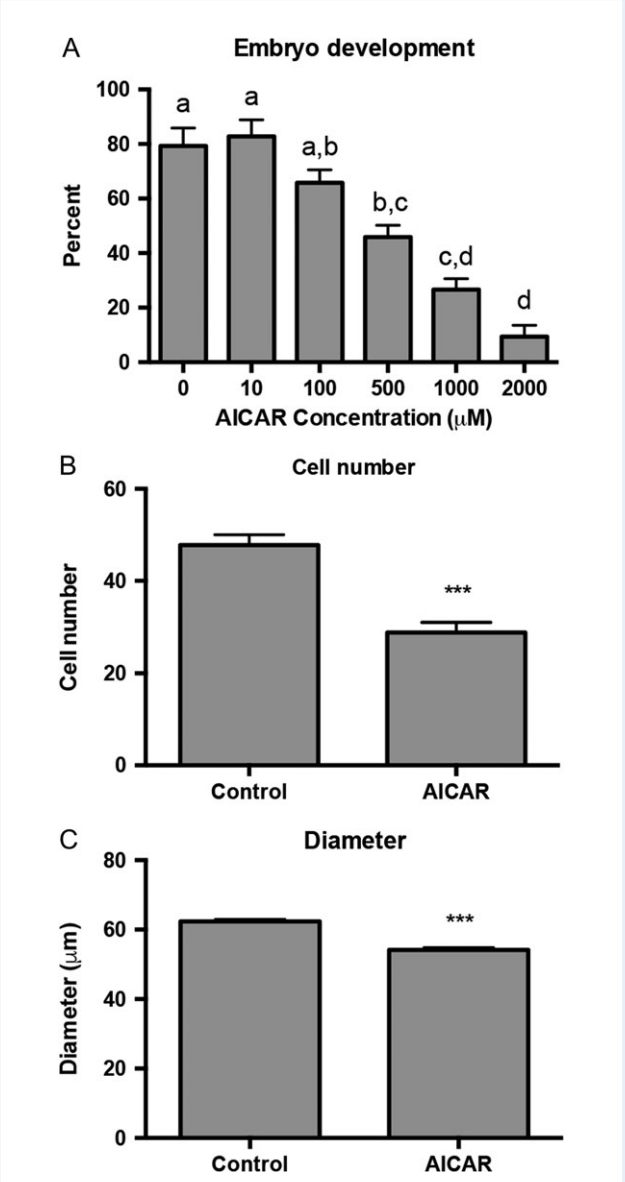

Figure 1 AICAR treatment at the 2-cell stage decreased development, blastocyst diameter and total cell counts. (**A**) Development to blastocyst after treatment with various doses of AICAR, $n = 5$, 133–148 embryos per dose. a,b,c,d Groups without letters in common are significantly different, $P < 0.001$. (**B**) Cell counts after culture for 48 h with 0 or 1000 μM AICAR, $n = 5$, with 92 embryos for control and 65 AICAR-treated embryos. ***$P < 0.001$. (**C**) Embryo diameter after culture for 48 h with 0 or 1000 μM AICAR, $n = 9$, with 317 for control and 333 for AICAR-treated embryos. ***$P < 0.001$.

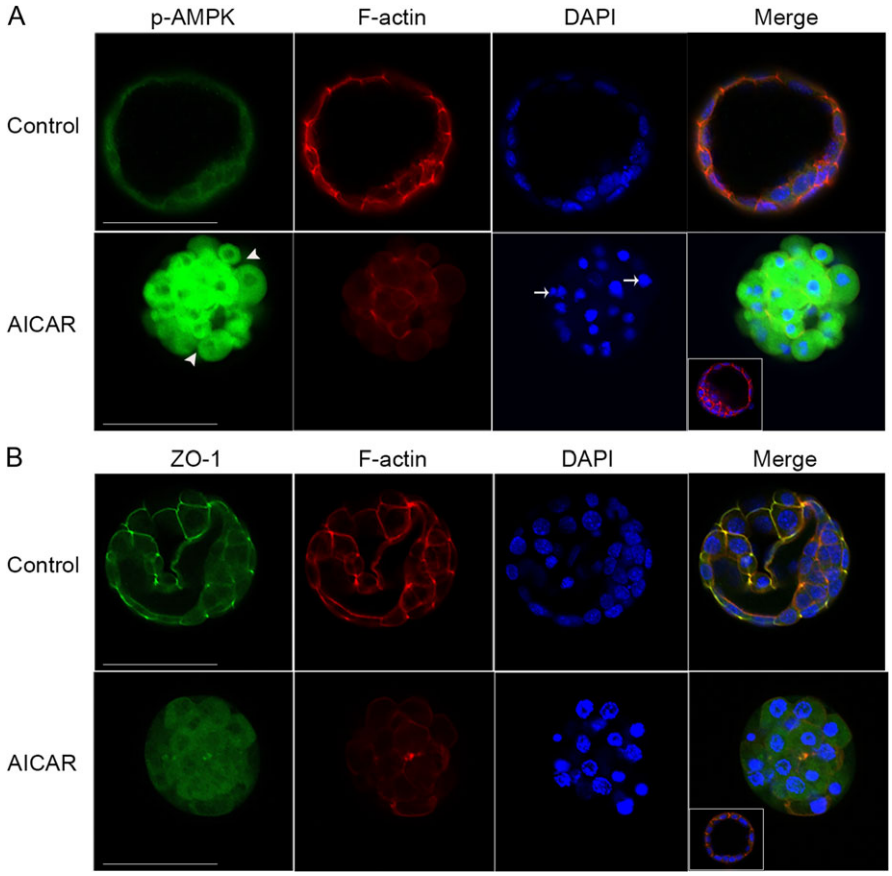

Figure 2 AICAR treatment increased detection of p-AMPK and decreased ZO1 (TJP1) localization to the cell membrane. (**A**) phospho-AMPK after 48 h culture of 2-cell embryos. Green panel shows p-AMPK fluorescence. Red is rhodamine-phalloidin staining of F-actin. Blue is DAPI-stained DNA. Merged figure shows color overlap. Arrowheads show evidence of loss of cell-to-cell contacts. Arrows show examples of condensed nuclei. Scale bar demonstrates 50 μM. Inset shows negative control with no primary antibody. (**B**) ZO1 (TJP1) after 48 h culture of 2-cell embryos. Green panel shows ZO1 fluorescence. Red is rhodamine-phalloidin staining of F-actin. Blue is DAPI-stained DNA. Yellow demonstrates overlap of ZO-1 and actin in the merged figure of the control embryos, which is missing in the AICAR-treated embryos. Scale bar demonstrates 50 μM. Inset shows negative control with no primary antibody.

Effects of AICAR Treatment on protein detection by western immunoblotting

AICAR treatment from the 2-cell stage significantly increased phosphorylated AMPK nearly 7-fold (Fig. 4A). CDX2 protein significantly decreased 4-fold in AICAR-treated embryos (Fig. 4B). However, E-cadherin protein (CDH1) was not affected by AICAR treatment (Fig. 4C). Uncropped blots are shown in Supplementary Fig. S2. In a preliminary analysis, we observed that AICAR tended to increase phosphorylation of ACC and decreased pS6 (Supplementary Fig. S3). However, pre-treatment with CC for 3 h prior to AICAR treatment did not alter phosphorylation of AMPK and ACC (Supplementary Fig. S4) and did not reverse the AICAR-stimulated pS6 decrease.

AICAR treatment decreased the expression of key blastocyst formation genes

When embryos were treated from the two-cell stage with 1000 μM AICAR, relative mRNA transcript levels encoding several blastocyst formation gene families were affected. *Cdx2*, *Aqp9* and *Atp1b1* mRNA levels were detected at significantly lower levels in AICAR-treated embryos, while *Gadd45a* mRNA was increased (Fig. 5). Levels of *Ocln*, *Cdh1*, *Atp1a1*, *Actb* and *Tjp1* mRNA were not significantly affected (Fig. 5).

AICAR treatment at the blastocyst stage caused some embryos to collapse and treatment was only partly reversible

About 23% blastocysts collapsed after incubation in 1000 μM AICAR for 9 h. All non-treated embryos remained at the blastocyst stage, while the median value of AICAR-treated embryos remaining blastocysts was 76.92%. After 9 h of incubation, control embryos were either frozen at −80°C or washed three times (sham control) and placed back into culture for an additional 24 h in drug free KSOM. AICAR-treated embryos were either frozen or washed three times in AICAR-free KSOM and separated into two drug free KSOM groups

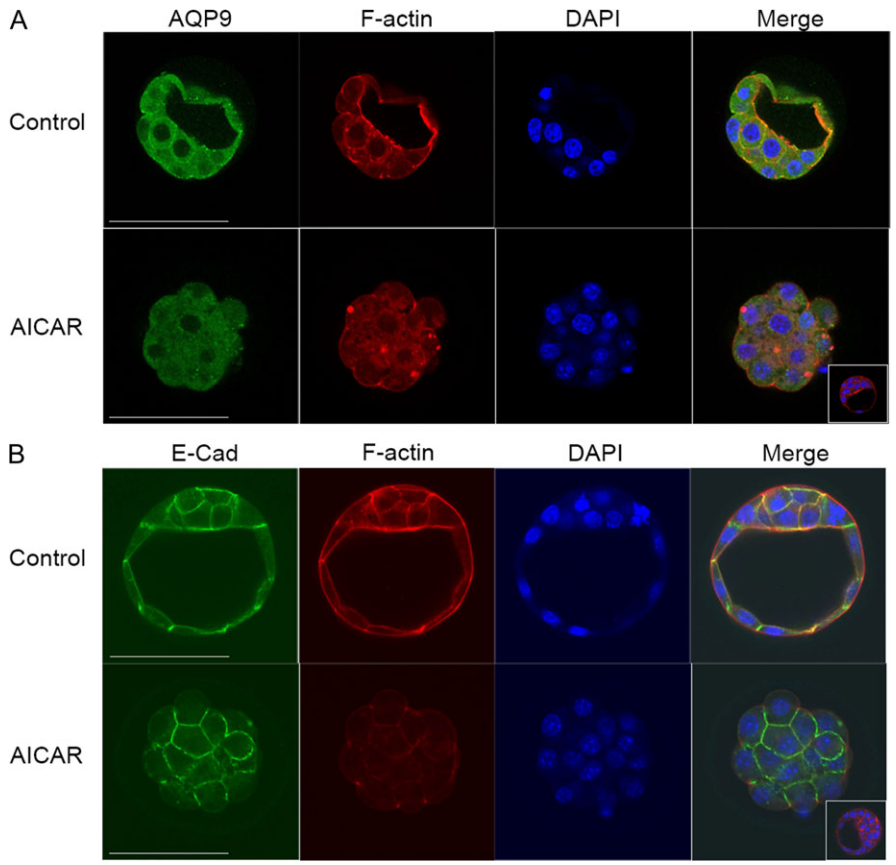

Figure 3 AICAR treatment decreased AQP9 but did not affect E-cadherin (CDH1) protein. (**A**) Aquaporin 9 (AQP9) after 48 h culture of 2-cell embryos. Green panel shows AQP9 fluorescence. Red is rhodamine-phalloidin staining of F-actin. Blue is DAPI-stained DNA. Merged figure shows color overlap, there is less overlap of AQP9 and actin in AICAR-treated compared to control embryos. Scale bar demonstrates 50 μM. Inset shows negative control with no primary antibody. (**B**) E-cadherin (CDH1) after 48 h culture of 2-cell embryos. Green panel shows CDH1 fluorescence. Red is rhodamine-phalloidin staining of F-actin. Blue is DAPI-stained DNA. Yellow demonstrates overlap of CDH1 and actin in the merged figure. There is a similar extent of overlap in both control embryos and AICAR-treated embryos. Scale bar demonstrates 50 μM. Inset shows negative control with no primary antibody.

according to their phenotype after 9 h of AICAR treatment: (1) blastocysts maintaining a cavity and (2) collapsed blastocysts. Examples of AICAR-treated embryos that collapsed are shown (asterisks, Fig. 6B). After 24 h of recovery culture, all control blastocysts remained blastocysts with a cavity. The median value of AICAR-treated embryos that initially had a cavity and maintained the cavity was 84.62%, and the median value of AICAR-treated embryos that had collapsed and recovered to generate a cavity was 56.67%. Embryo diameters were measured at the 0 , 9 and 24 h of recovery time points (Fig. 6A). At 9 h, the AICAR-treated group had significantly smaller diameters than controls at 9 h (61.26 ± 0.92 versus 76.05 ± 1.27 μM, $P < 0.05$). After 24 h of recovery culture, controls expanded up to an average of 103.90 ± 2.16 μM and were significantly different from all other groups. Following 24 h of washout of AICAR, embryos that remained blastocysts after 9 h of AICAR treatment (aibl) and those that initially collapsed but recovered to blastocyst after 24 h (ai rec) had similar diameters, 67.98 ± 2.15 and 72.43 ± 0.66 μM, respectively. Aicoll were embryos that collapsed after 9 h AICAR treatment and never recovered, and were significantly smaller (53.19 ± 0.62 μM) than either aibl or ai rec blastocysts. Representative photomicrographs from 9 and 24 h periods are shown in Fig. 6B. After 24 h of recovery, embryos were frozen for further analysis as pools of those that (1) maintained a blastocyst cavity throughout (aibl); (2) those that initially collapsed but recovered to become expanded blastocysts (ai rec); and (3) those that remained collapsed (aicoll) and showed no recovery from treatment.

CDX2 protein levels are significantly reduced in AICAR treated embryos

CDX2 immunofluorescence intensity decreased after 1000 μM AICAR treatment (Fig. 7A amd B), while F-actin fluorescence intensity was not significantly lower in AICAR treated embryos compared to control embryos (Fig. 7C).

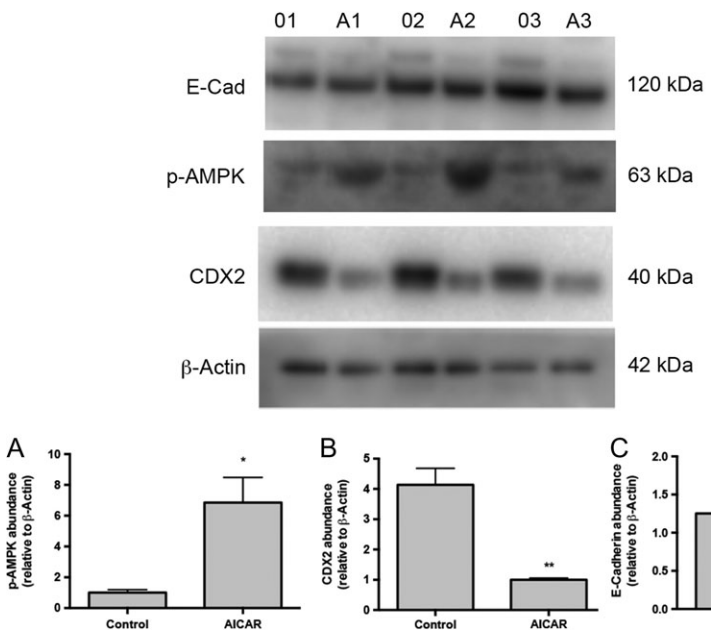

Figure 4 AICAR treatment increased detection of p-AMPK and decreased CDX2 by Western blot. Top panel shows Western blots, Control (01, 02, 03) and AICAR-treated (A1, A2, A3) embryos. β-actin shows equal protein loading, not significantly different between control and AICAR-treated embryos. (**A**) p-AMPK after 48 h culture of 2-cell embryos. There was $n = 3$ independent sample pools (30 embryos per pool). Control (01, 02, 03) and AICAR-treated (A1, A2, A3) embryos were significantly different, $^{*}P < 0.05$. (**B**) CDX2 after 48 h culture of 2-cell embryos. Control (01, 02, 03) and AICAR-treated (A1, A2, A3) embryos were significantly different, $^{**}P < 0.01$. (**C**) CDH1 after 48 h culture of 2-cell embryos. Control (01, 02, 03) and AICAR-treated (A1, A2, A3) embryos were not significantly different.

AICAR treatment of blastocysts caused a reduction of some blastocyst formation gene mRNA levels

Due to the much larger diameter of the 24 h control (Con 24) embryos, we analyzed relative mRNA levels only among: (1) 0 h controls, (2) 9 h of treatment and (3) 24 h of recovery after AICAR treatment groups. *Cdx2* abundance increased from time 0 to 9 h in controls, but was significantly decreased in 9 h AICAR-treated embryos (Fig. 8). Even after 24 h of recovery time, *Cdx2* mRNA levels in AICAR-treated blastocysts (aibl and ai rec) had not recovered to Con 9 h levels. Embryos that remained collapsed (aicoll) did not show any recovery in *Cdx2* mRNA levels. Like *Cdx2*, *Cdh1* was highest in Con 9 h. AICAR-treated embryos treated for 9 h had significantly lower *Cdh1* mRNA than Con 9 h embryos. However, after 24 h of recovery, AICAR-treated embryos that were blastocysts (aibl and ai rec) had similar levels of *Cdh1* transcript abundance as Con 9 h, while aicoll embryos did not. The aicoll group had the lowest level of *Aqp9* mRNA. *Atp1b1* mRNA levels increased from time 0 in Con 9 h embryos that continued to expand, while AICAR 9 h embryos had significantly lower *Atp1b1* mRNA levels than Con 9 h. After 24 h of recovery, aibl and ai rec blastocysts displayed a modest increase in *Atp1b1* mRNA levels while embryos in the aicoll group did not. Only the aicoll group embryos contained significantly lower *Ocln* levels than Con 9 h expanded blastocysts. *Tjp1*, *Gadd45a*, *Actb* and *Atp1a1* mRNA levels did not significantly differ between times, treatments and stages. This outcome is significant as while the aicoll group overall showed very limited if any recovery from treatment, it was possible to detect mRNA from these embryos for the blastocyst formation gene family members. Thus, while these embryos did not recover from treatment, they were still intact.

AICAR treatment caused embryos to become more permeable in a tight junction permeability assay

Blastocysts incubated in AICAR for 9 h displayed a significant 2.8-fold increase in permeability to 40 kDa FITC-Dextran (50.3 ± 0.5%). Control embryos were the least permeable (18.1 ± 5.3%), while positive control EGTA-treated embryos were intermediate (30.7 ± 6.5%, Fig. 9A). Representative bright-field and FITC-filter images are shown in Fig. 9B.

AICAR treatment did not affect total embryo ATP content

There were no significant differences in total ATP content between control embryos or those treated with AICAR for 48 h (data not shown).

Discussion

Applying 1000 μm AICAR, an AMPK activator, to mouse 2-cell embryos reduced the number of embryos that developed to the blastocyst stage at 48 h. This was confirmed with other known

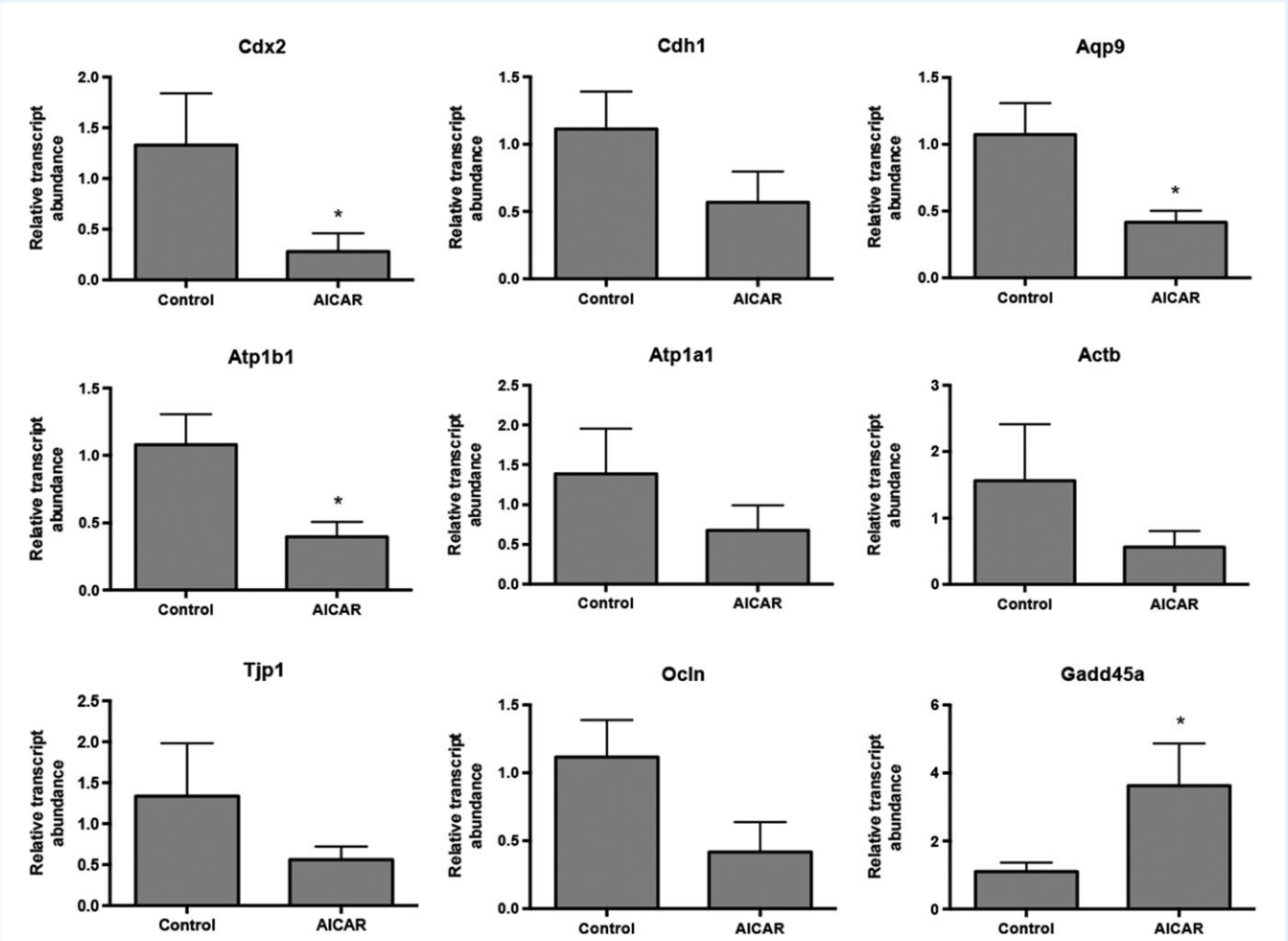

Figure 5 Real-time PCR analysis of mRNA levels of 2-cell embryos cultured for 48 h with AICAR. *Cdx2*, *Cdh1*, *Aqp9*, *Atp1b1*, *Atp1a1*, *Actb*, *Tjp1*, *Ocln* and *Gadd45a* are shown. Significant differences between control and AICAR-treated embryos are signified by $^*P < 0.05$. Mean ± SEM are depicted. There was $n = 3$–5 independent samples.

activators of AMPK, metformin and phenformin. The effective dose of metformin in our study was 1000 μM, similar to that used in other studies in tissues as well as oocytes and embryos (0.5–2 mM, Zhou *et al.*, 2001; Meley *et al.*, 2006; Bilodeau-Goeseels *et al.*, 2011, 2014; Bolnick *et al.*, 2016). Similarly, metformin inhibited mouse blastocyst development at 100 μg/ml (~600 μM) in an earlier study (Bedaiwy *et al.*, 2001). Maximal blood concentrations in diabetic humans treated with metformin are recommended to be lower than 2.5 mg/l (19 μM, Graham *et al.*, 2011). In a study performed in mice, maximal serum concentrations of metformin were 52 μM after an oral dose of 50 mg/kg, but accumulated at higher concentrations in some tissues (Wilcock and Bailey, 1994). In our study, phenformin had a greater effect than metformin on embryo development, in accordance with similar studies with mid-gestation mouse embryos (Denno and Sadler, 1994) and killed preimplantion embryos at doses above 100 μM. Diminishing doses blocked mouse embryo development at later stages. In our study, the minimum effective dose of phenformin for blocking blastocyst formation was 10 μM. AICAR reduced the embryo diameter as well as embryo cell number. This concentration (1000 μM) was similar to doses of AICAR that stimulate meiosis in mouse oocytes (Downs *et al.*, 2002) and those used to activate AMPK in other studies (Mayes *et al.*, 2007; Yokoyama *et al.*, 2011; Ding *et al.*, 2013; Xie *et al.*, 2013). Treated embryos in our study arrested primarily at the morula stage. Activation of AMPK induces cell-cycle arrest in some cancer cell lines (reviewed in Hardie, 2011). AICAR treatment of blastocysts frequently resulted in blastocyst collapse, blastomere rounding and loss of cell-to-cell contacts. Furthermore, embryos treated from the two-cell stage onwards displayed nuclei that were condensed, suggestive of initiation of apoptosis seen in other cell types after AMPK activation (Okoshi *et al.*, 2008). Confocal microscopy and Western blot analysis demonstrated that AICAR potently stimulated phosphorylation of AMPK. Western blot analysis showed that AICAR tended to increase phosphorylation of ACC and decrease pS6 levels. AICAR and metformin treatment have been shown to decrease pS6 previously (Tosca *et al.*, 2007; Guo *et al.*, 2009).

We found that the AMPK inhibitor, CC, did not inhibit blastocyst development at normally used concentrations (5–10 μM, Chen *et al.*, 2006; Bilodeau-Goeseels *et al.*, 2011, 2014; Xie *et al.*, 2013) and only

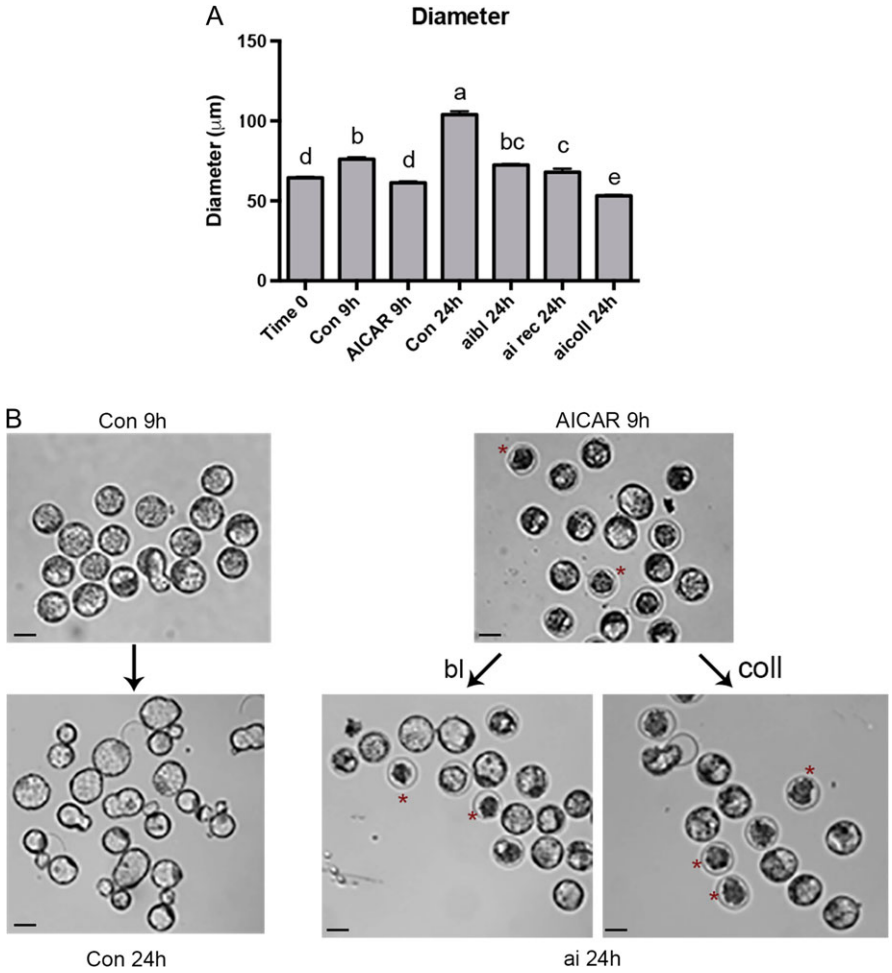

Figure 6 Recovery of Blastocysts following 9 h of AICAR Treatment. (**A**) Embryo diameter at time 0, 9 h of treatment or 24 h of recovery. $n = 5–8$ with 96–563 embryos per group. a,b,c,d,e Groups that do not have a letter in common are significantly different, $P < 0.05$. (**B**) A photomicrograph of control or AICAR-treated embryos of one experiment is representatively shown after 9 h treatment and then after 24 h of recovery in drug free medium (Con 24 h and ai 24 h). At 9 h, AICAR embryos were divided into those that remained blastocysts and those that collapsed. AICAR-treated embryos are darker and less expanded than controls. Examples of collapsed embryos are shown with red asterisks. Scale bar demonstrates 50 μM. Time 0, (control at start of experiment); Con 9 h, untreated controls cultured for 9 h; AICAR 9 h, (blastocysts treated with AICAR for 9 h); Con 24 h, (controls cultured for 24 h in drug free medium); aibl 24 h, (AICAR treated embryos that did not collapse after 9 h treatment); ai rec 24 h, (AICAR treated embryos which initially collapsed that did recover after 24 h in drug free medium); aicoll 24 h, (AICAR treated collapsed blastocysts that did not recover after 24 h in drug free medium).

became inhibitory at 100 μM. CC did not reverse the inhibitory effect of AICAR treatment on development, or on phosphorylation of AMPKα and acetyl CoA carboxylase (pACC), nor block the decrease in pS6. Previous studies have shown a reduction in pACC in hepatocytes (Zhou *et al.*, 2001) and in mouse oocytes following CC treatment (Chen *et al.*, 2006). However, AICAR reduced oocyte maturation yet failed to increase pAMPK in bovine oocytes (Bilodeau-Goeseels *et al.*, 2011) or to increase pACC in bovine and porcine oocytes (Bilodeau-Goeseels *et al.*, 2011, 2014). In addition, CC did not affect pACC in porcine oocytes (Bilodeau-Goeseels *et al.*, 2014) and CC failed to block pAMPK and pACC in another study (Meley *et al.*, 2006), which was dependent on culture conditions. Further, in a study by Guo *et al.* (2009), CC was able to block the effects of AICAR on pACC but did not appear to block AICAR-mediated reduction in phosphorylation of pS6. Metformin treatment also reduces S6 phosphorylation and this was not blocked by CC or AMPK siRNA knockdown (Klubo-Gwiezdzinska *et al.*, 2012). This may demonstrate that both AICAR and CC may affect embryo development by AMPK-dependent and AMPK-independent mechanisms.

Messenger RNA was decreased for both *Atp1b1* and *Aqp9* following AICAR treatment, which are both required for expansion of the blastocyst (Barcroft *et al.*, 2003; Madan *et al.*, 2007). AICAR treatment decreased *Aqp9* mRNA levels over 12 h in a previous study (Yokoyama *et al.*, 2011). Embryos treated with AICAR from the two-cell stage had reduced *Aqp9* mRNA and decreased AQP9 fluorescence intensity at the cell membrane. *Atp1b1* mRNA was significantly

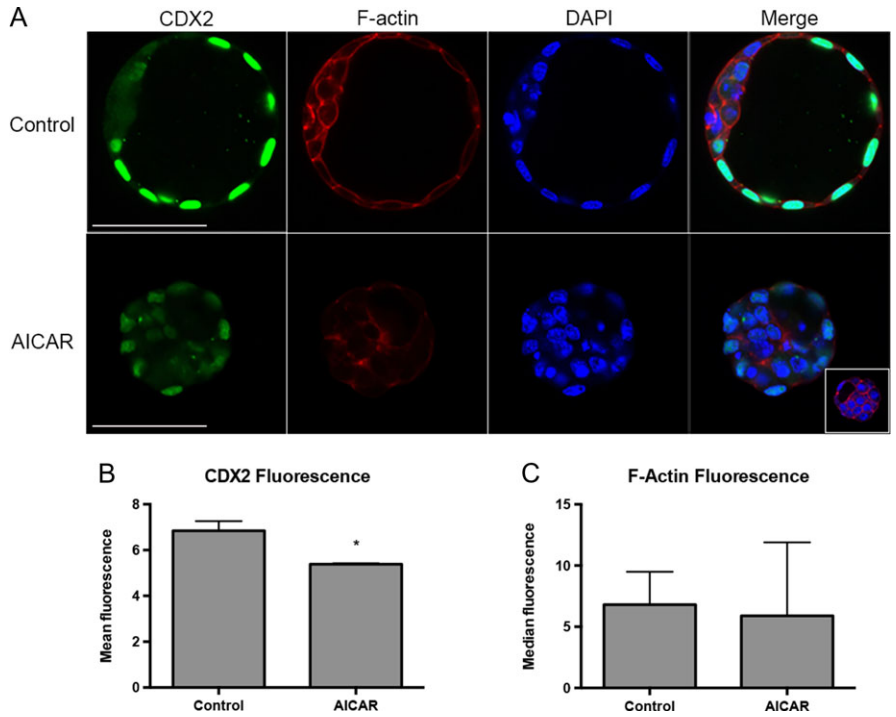

Figure 7 AICAR treatment of blastocysts decreased immunofluorescent detection of CDX2 protein. (**A**) CDX2 after 48 h culture of 2-cell embryos. Green panel shows CDX2 fluorescence. Red is rhodamine-phalloidin staining of F-actin. Blue is DAPI-stained DNA. Merged figure shows color overlap. CDX2 is confined to the nuclei of TE in control embryos. (**B**) Quantification of CDX2 staining in relative fluorescence units, $n = 3$ with a total of 49 and 50 embryos. CDX2 protein is lower in AICAR-treated embryos, $P < 0.05$. (**C**) Quantification of F-actin staining in relative fluorescent units, $n = 3$ with a total of 49 and 50 embryos. F-actin intensity is not different between control and AICAR-treated embryos. Scale bar demonstrates 50 μM. Inset shows negative control with no primary antibody.

lower in embryos treated continuously from the two-cell stage and in blastocysts treated for only 9 h. Blastocysts which recovered from AICAR treatment regained *Atp1b1* expression while those that remained collapsed did not. Interestingly, *Atp1a1* mRNA was not significantly decreased by AICAR treatment. This may be related to the fact that *Atp1a1* knockout embryos (Barcroft *et al.*, 2004) can become blastocysts while *Atp1b1* knockout embryos cannot (Madan *et al.*, 2007). This suggests that the β-1 subunit of Na+/K+ ATPase may be the more critical partner, serving as a rate limiting step for successful cavitation. Studies have demonstrated that *Atp1a1* levels are substantial during mouse preimplantation development and are thus not likely rate limiting with regards to providing appropriate Na+/K+ -ATPase activity to fuel blastocyst formation (Watson *et al.*, 1990; Barcroft *et al.*, 2004). It is also possible that the reduced *Atp1b1* mRNA translated to reduced protein expression in the TE, which is also required for normal tight junction formation.

TJP1, OCLN and CDH1 are all key proteins that collaborate together in the mechanisms controlling tight junction formation and establishment of the blastocyst. Fluorescence intensity of tight junction protein (TJP1, ZO-1) was decreased at the membrane in AICAR-treated embryos though it was not affected at the mRNA level. *Ocln* mRNA decreased after AICAR treatment, and was significantly decreased in blastocysts that collapsed after recovery in drug-free medium. We have previously reported decreased ZO1 and occludin protein in ouabain (Na+/K+ ATPase inhibitor and possible ligand) treated embryos (Violette *et al.*, 2006). AICAR-treated blastocysts had increased uptake of FITC-labeled dextran compared to controls, which indicates that tight junctional permeability increased in treated embryos. About 50% of AICAR-treated embryos were permeable to 40 kDa FITC-Dextran compared to 18% of untreated controls. The consequences would be that AICAR-treated embryos would have more difficulty in maintaining an expanded blastocyst cavity and in fact would be unlikely to cavitate if the deficit persisted, as we observed. Blastocyst cavity formation relies on a TE tight junctional seal forming to prevent trapped blastocyst fluid from leaking out from between TE cells resulting in blastocyst collapse (Watson and Kidder, 1988; Betts *et al.*, 1998; MacPhee *et al.*, 2000; Watson *et al.*, 2004). Although AMPK activation increases tight junction assembly in some epithelial cells and decreases paracellular permeability (Zhang *et al.*, 2006; Zheng and Cantley, 2007), by contrast, activation of AMPK can also increase tight junction width and paracellular permeability in salivary cells (Ding *et al.*, 2013).

E-cadherin was not affected at either the mRNA or protein level in AICAR treated embryos. *Cdh1* mRNA did however decrease in blastocysts treated for 9 h with AICAR and remained low in embryos that remained collapsed. F-actin fluorescence was visibly decreased at cell cortical regions although no change in the level of *Actb* mRNA or protein was observed in AICAR treated embryos. F-actin results from the polymerization of any of three types of actin; alpha, beta or gamma. AMPK activation can decrease actin assembly in endothelial cells

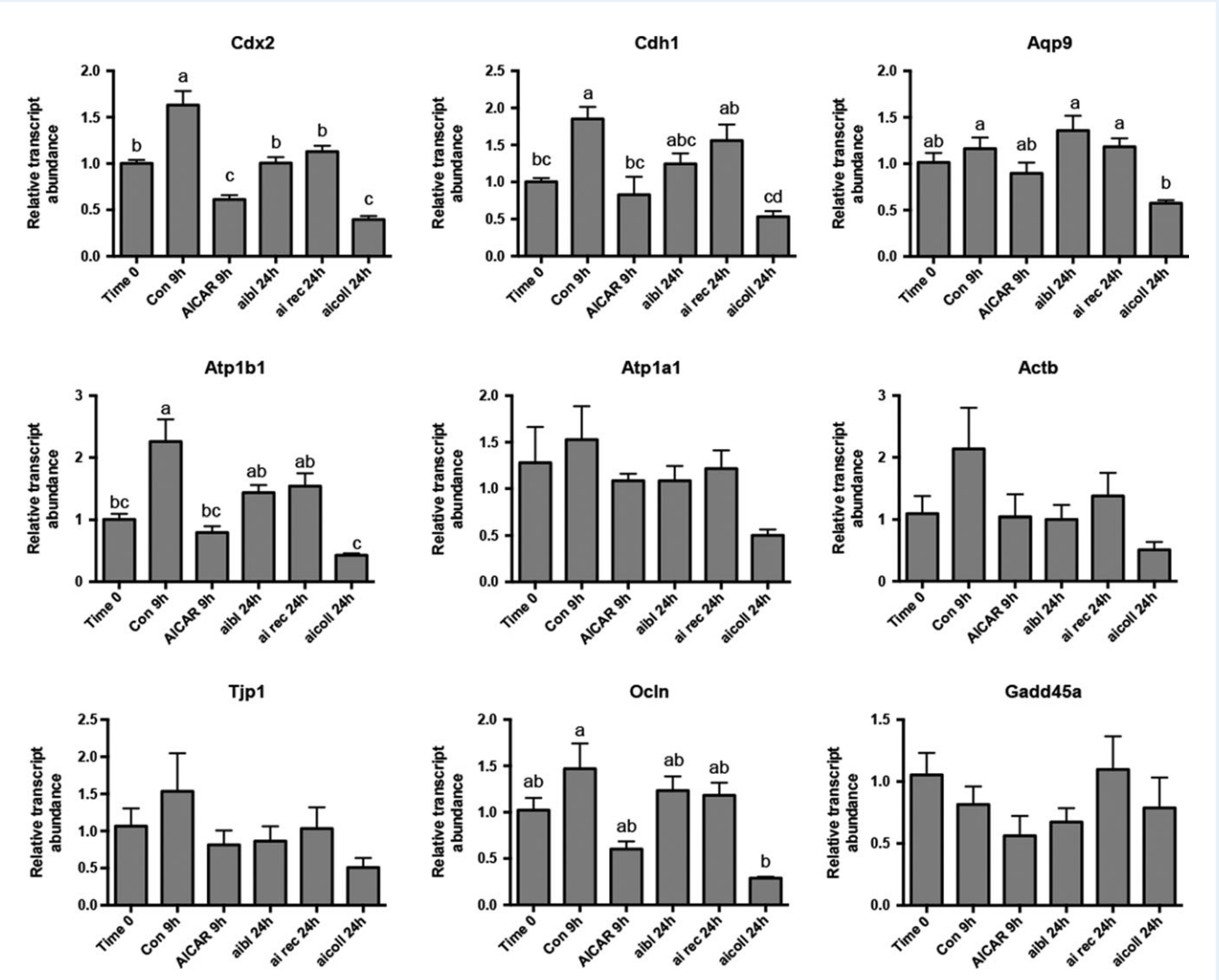

Figure 8 Real-time PCR analysis of blastocyst mRNA levels at time 0, 9 h of treatment or 24 h of recovery. *Cdx2*, *Cdh1*, *Aqp9*, *Atp1b1*, *Atp1a1*, *Actb*, *Tjp1*, *Ocln* and *Gadd45a* are shown. Significant differences between control and AICAR-treated embryos are signified by a,b,c,d $P < 0.05$. There were $n = 4$ replicates. Time 0, (control at start of experiment); Con 9 h, untreated controls; AICAR 9 h, (blastocysts treated with AICAR for 9 h); Con 24 h, (sham controls cultured for 24 h in drug free medium); aibl 24 h, (AICAR treated embryos that did not collapse after 9 h treatment after a further 24 h in drug free medium); ai rec 24 h, (AICAR treated collapsed blastocyst that did recover after 24 h in drug free medium); aicoll 24 h, (AICAR treated collapsed blastocysts that did not recover after 24 h in drug free medium).

(Blume *et al.*, 2007) and mesenchymal cancers displayed decreased F-actin after AMPK activation along with decreased markers of invasiveness (Chou *et al.*, 2014).

CDX2 is an important transcription factor and marker for TE cell fate determination and TE differentiation. CDX2 protein was significantly decreased in AICAR-treated blastocysts, as well as at the mRNA level in both experiments. Reduced CDX2 protein was previously seen in embryos and trophectoderm stem cells treated with AICAR or subjected to hyperosmolar stress (Xie *et al.*, 2013). Bovine embryos that resulted in pregnancy had higher expression of *Cdx2* mRNA than those that did not result in pregnancy (El-Sayed *et al.*, 2006). Furthermore, mouse *Cdx2* knockout embryos do not give rise to live births (Chawengsaksophak *et al.*, 1997). Collectively, a decline in CDX2 expression following AICAR treatment is a strong indicator of expected declining developmental competence.

AMPK increases expression of GADD45A in some cells (Chen *et al.*, 2015). Transcription of *Gadd45a* is stimulated by oxidative stress and causes cell cycle arrest at G2/M phase (Furukawa-Hibi *et al.*, 2002). Thus, it may be responsible for halting embryonic cell proliferation. Gadd45a$^{-/-}$ mice are more susceptible to mammary tumors and tumors had less expression of apoptosis and senescence markers (Tront *et al.*, 2006). In our experiments, G*add45a* mRNA was increased in embryos treated 48 h from the two-cell stage but not in blastocysts treated for a shorter time. This may suggest that after a long period of AMPK activation, increased *Gadd45a* may lead some embryos to become senescent.

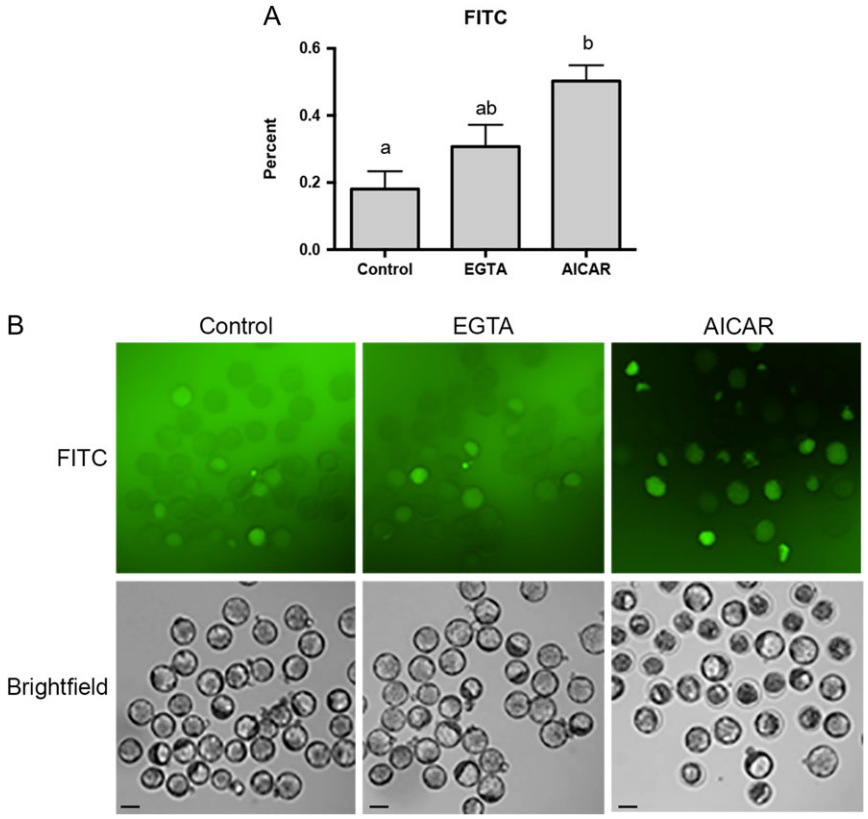

Figure 9 AICAR treatment increased uptake of 40 kDa FITC-Dextran in blastocysts. (**A**) Significant differences in dye uptake between control, EGTA and AICAR-treated embryos are signified by a,b $P < 0.05$. There was $n = 5$ replicates. (**B**) Representative bright-field and FITC-filter photographs for control, EGTA and AICAR. Scale bar demonstrates 50 μM.

Together, our results demonstrate that AMPK is likely a critical regulatory nexus for ensuring that blastocyst formation unfolds as it should. The outcomes also alert us to the possibility of residual downstream negative effects of metformin treatment on embryonic developmental competence. Further studies should investigate this possibility to better inform fertility treatments and protocols using metformin to treat PCOS and type II diabetes.

Supplementary data

Supplementary data are available at *Molecular Human Reproduction*.

Acknowledgments

We would like to thank Dr Christine Bell, Rucha Khandekar, Reshvinder Dhillon and Kylie Crocker for their assistance with embryo collections.

Authors' roles

M.D.C. and A.J.W. conceived the experiments. M.D.C. and N.A.E. carried out the experiments and performed data analysis. M.D.C., N.A.E. and A.J.W. participated in manuscript drafting. D.H.B. was involved with critical discussion and final drafting.

Funding

Research supported by a Canadian Institutes of Health Research operating grant MOP 130396 'Culture Stress and the pre-implantion embryo: implications for single embryo transfer' to D.H.B. and A.J.W. N.A.E. is supported by a Natural Sciences and Engineering Research Council of Canada Doctoral Graduate Scholarship.

Conflict of interest

Authors state that they have no potential conflicts of interest to declare.

References

Barcroft LC, Offenberg H, Thomsen P, Watson AJ. Aquaporin proteins in murine trophectoderm mediate transepithelial water movements during cavitation. *Dev Biol* 2003;**256**:342–354.

Barcroft LC, Moseley AE, Lingrel JB, Watson AJ. Deletion of the Na/K-ATPase alpha1-subunit gene (Atp1a1) does not prevent cavitation of the preimplantation mouse embryo. *Mech Dev* 2004;**121**:417–426.

Bedaiwy MA, Miller KF, Goldberg JF, Nelson D, Falcone T. Effect of metformin on mouse embryo development. *Fertil Steril* 2001;**76**:1078–1079.

Bell CE, Watson AJ. p38 MAPK regulates cavitation and tight junction function in the mouse blastocyst. *PLoS One* 2013;**8**:e59528.

Bertoldo MJ, Guibert E, Faure M, Rame C, Foretz M, Viollet B, Dupont J, Froment P. Specific deletion of AMP-activated protein kinase (α1 AMPK) in murine oocytes alters junctional protein expression and mitochondrial physiology. *PLoS One* 2015;**10**:e0119680.

Betts DH, Barcroft LC, Watson AJ. Na/K-ATPase-mediated 86Rb+ uptake and asymmetrical trophectoderm localization of alpha1 and alpha3 Na/K-ATPase isoforms during bovine preattachment development. *Dev Biol* 1998;**197**:77–92.

Bilodeau-Goeseels S, Panich PL, Kastelic JP. Activation of AMP-activated kinase may not be involved in AICAR- and metformin-mediated meiotic arrest in bovine denuded and cumulus-enclosed oocytes in vitro. *Zygote* 2011;**19**:97–106.

Bilodeau-Goeseels S, Magyara N, Collignon C. Characterization of the effects of metformin on porcine oocyte meiosis and on AMP-activated protein kinase activation in oocytes and cumulus cells. *Zygote* 2014;**22**:275–285.

Blume C, Benz PM, Walter U, Ha J, Kemp BE, Renne T. AMP-activated protein kinase impairs endothelial actin cytoskeleton assembly by phosphorylating vasodilator-stimulated phosphoprotein. *J Biol Chem* 2007;**282**:4601–4612.

Bolnick A, Abdulhasan M, Kilburn B, Xie Y, Howard M, Andresen P, Shamir AM, Dai J, Puscheck EE, Rappolee DA. Commonly used fertility drugs, a diet supplement, and stress force AMPK-dependent block of stemness and development in cultured mammalian embryos. *J Assist Reprod Genet* 2016;**33**:1027–1039.

Carling D, Clarke PR, Zammit VA, Hardie DG. Purification and characterization of the AMP-activated protein kinase. Copurification of acetyl-CoA carboxylase kinase and 3-hydroxy-3-methylglutaryl-CoA reductase kinase activities. *Eur J Biochem* 1989;**186**:129–136.

Chawengsaksophak K, James R, Hammond VE, Köntgen F, Beck F. Homeosis and intestinal tumours in Cdx2 mutant mice. *Nature* 1997;**386**:84–87.

Chen J, Hudson E, Chi MM, Chang AS, Moley KH, Hardie DG, Downs SM. AMPK regulation of mouse oocyte meiotic resumption in vitro. *Dev Biol* 2006;**291**:227–238.

Chen H, Wang JP, Santen RJ, Yue W. Adenosine monophosphate activated protein kinase (AMPK), a mediator of estradiol-induced apoptosis in long-term estrogen deprived breast cancer cells. *Apoptosis* 2015;**20**:821–830.

Chou CC, Lee KH, Lai IL, Wang D, Mo X, Kulp SK, Shapiro CL, Chen CS. AMPK reverses the mesenchymal phenotype of cancer cells by targeting the Akt-MDM2-Foxo3a signalling axis. *Cancer Res* 2014;**74**:4783–4795.

Corton JM, Gillespie JG, Hawley SA, Hardie DG. 5-amidoimidazole-4-carboxamide ribonucleoside: a specific method for activating AMP-activated protein kinase in intact cells. *Eur J Biochem* 1995;**229**:558–565.

da Silva Xavier G, Leclerc I, Salt IP, Doiron B, Hardie DG, Kahn A, Rutter GA. Role of AMP-activated protein kinase in the regulation by glucose of islet beta cell gene expression. *Proc Nat Acad Sci* 2000;**97**:4023–4028.

Denno KM, Sadler TW. Effects of the biguanide class of oral hypoglycemic agents on mouse embryogenesis. *Teratology* 1994;**49**:260–266.

Ding C, Li L, Su YC, Xiang RL, Cong X, Yu HK, Li SL, Wu LL, Yu GY. Adiponectin increases secretion of the rat submandibular gland via adiponectin receptors-mediated AMPK signalling. *PLoS One* 2013;**8**:e63878.

Downs SM, Hudson ER, Hardie DG. A potential role for AMP-activated protein kinase in meiotic induction in mouse oocytes. *Dev Biol* 2002;**245**:200–212.

Edwards NA, Watson AJ, Betts DH. P66Shc, a key regulator of metabolism and mitochondrial ROS production, is dysregulated by mouse embryo culture. *Mol Hum Reprod* 2016;**22**:634–647.

El-Sayed A, Hoelker M, Rings F, Salilew D, Jennen D, Tholen E, Sirard MA, Schellander K, Tesfaye D. Large-scale transcriptional analysis of bovine embryo biopsies in relation to pregnancy success after transfer to recipients. *Physiol Genomics* 2006;**28**:84–96.

Eng GS, Sheridan RA, Wyman A, Chi MM, Bibee KP, Jungheim ES, Moley KH. AMP kinase activation increases glucose uptake, decreases apoptosis, and improves pregnancy outcome in embryos exposed to high IGF-I concentrations. *Diabetes* 2007;**56**:2228–2234.

Fleming TP, McConnell J, Johnson MH, Stevenson BR. Development of tight junctions de novo in the mouse early embryo: Control of assembly of the tight junction-specific protein, ZO-1. *J Cell Biol* 1989;**108**:1407–1418.

Fong B, Watson PH, Watson AJ. Mouse preimplantation embryo responses to culture medium osmolarity include increased expression of CCM2 and p38 MAPK activation. *BMC Dev Biol* 2007;**7**:2.

Furukawa-Hibi Y, Yoshida-Araki K, Ohta T, Ikeda K, Motoyama N. FOXO forkhead transcription factors induce G(2)-M checkpoint in response to oxidative stress. *J Biol Chem* 2002;**277**:26729–26732.

Graham GG, Punt J, Arora M, Day RO, Doogue MP, Duong JK, Furlong TJ, Greenfield JR, Greenup LC, Kirkpatrick CM *et al*. Clinicopharmacokinetics of Metformin. *Clin Pharmacokin* 2011;**50**:81–98.

Guo D, Hildebrandt IJ, Prins RM, Soto H, Mazzotta MM, Dang J, Czernin J, Shyy JY-J, Watson AD, Phelps M *et al*. The AMPK agonist AICAR inhibits the growth of EGFRvIII-expressing glioblastomas by inhibiting lipogenesis. *Proc Natl Acad Sci USA* 2009;**106**:12932–12937.

Hardie DG. AMP-activated protein kinase: an energy sensor that regulates all aspects of cell function. *Genes Dev* 2011;**25**:1895–1908.

Hardie DG, Ross FA, Hawley SA. AMPK: a nutrient and energy sensor that maintains energy homeostasis. *Nat Rev Mol Cell Biol* 2012;**13**:251–262.

Kim J, Gye MC, Kim MK. The role of occludin, a tight junction protein, in blastocoel formation, and the paracellular permeability and differentiation of trophectoderm in preimplantation mouse embryo. *Mol Cell* 2004;**17**:248–254.

Klubo-Gwiezdzinska J, Jensen K, Costello J, Patel A, Hoperia V, Bauer A, Burman KD, Wartofsky L, Vasko V. Metformin inhibits growth and decreases resistance to anoikis in medullary thyroid cancer cells. *Endocr Relat Cancer* 2012;**19**:447–456.

Liu X, Chhipa RR, Pooyaa S, Wortman M, Yachyshin S, Chow LML, Kumar A, Zhou X, Sun Y, Quinn B *et al*. Discrete mechanisms of mTOR and cell cycle regulation by AMPK agonists independent of AMPK. *Proc Nat Acad Sci USA* 2014;**111**:E435–E444.

Liu Y, Wan Q, Guan Q, Gao L, Zhao J. High-fat diet feeding impairs both the expression and activity of AMPKa in rats' skeletal muscle. *Biochem Biophys Res Comm* 2006;**339**:701–707.

Louden ED, Luzzo KM, Jimenez PT, Chi T, Chi M, Moley KH. TallyHO obese female mice experience poor reproductive outcomes and abnormal blastocyst metabolism that is reversed by metformin. *Reprod Fertil Dev* 2014;**27**:31–39.

MacPhee DJ, Jones DH, Barr KJ, Betts DH, Watson AJ, Kidder GM. Differential involvement of Na(+),K(+)-ATPase isozymes in preimplantation development of the mouse. *Dev Biol* 2000;**222**:486–498.

Madan P, Rose K, Watson AJ. Na/K-ATPase beta1 subunit expression is required for blastocyst formation and normal assembly of trophectoderm tight junction-associated proteins. *J Biol Chem* 2007;**282**:12127–12134.

Mayes MA, Laforest MF, Guillemette C, Gilchrist RB, Richard FJ. Adenosine 5'-monophosphate kinase-activated protein kinase (PRKA) activators delay meiotic resumption in porcine oocytes. *Biol Reprod* 2007;**76**:589–597.

Meley D, Bauvy C, Houben-Weerts JH, Dubbelhuis PF, Helmond MT, Codogno P, Meijer AJ. AMP-activated protein kinase and the regulation of autophagic proteolysis. *J Biol Chem* 2006;**281**:34870–34879.

Nestler JE, Jakubowicz DJ, Evans WS, Pasquali R. Effects of metformin on spontaneous and clomiphene-induced ovulation in the polycystic ovary syndrome. *N Engl J Med* 1998;**338**:1876–1880.

Okoshi R, Ozaki T, Yamamoto H, Ando K, Koida N, Ono S, Koda T, Kamijo T, Nakagawara A, Kizaki H. Activation of AMP-activated protein kinase induces p53-dependent apoptotic cell death in response to energetic stress. *J Biol Chem* 2008;**283**:3979–3987.

Palomba S, Falbo A, La Sala GB. Metformin and gonadotropins for ovulation induction in patients with polycystic ovary syndrome: a systematic review with meta-analysis of randomized controlled trials. *Reprod Biol Endocrinol* 2014;**12**. doi:10.1186/1477-7827-12-3.

Pikiou O, Vasilaki V, Leondaritis G, Vamvakopoulos N, Messinis IE. Effects of metformin on fertilisation of bovine oocytes and early embryo development: possible involvement of AMPK3-mediated TSC2 activation. *Zygote* 2013;**23**:58–67.

Pfaffl MW. A new mathematical model for relative quantification in real-time RT-PCR. *Nucleic Acids Res* 2001;**25**:e45.

Ratchford AM, Chang AS, Chi MM, Sheridan R, Moley KH. Maternal diabetes adversely affects AMP-kinase activity and cellular metabolism in murine oocytes. *Am J Physiol Metab* 2007;**293**:E1198–E1206.

Strumpf D, Mao CA, Yamanaka Y, Ralston A, Chawengsaksophak K, Beck F, Rossant J. Cdx2 is required for correct cell fate specification and differentiation of trophectoderm in the mouse blastocyst. *Development* 2005;**132**:2093–2102.

Tang T, Glanville J, Orsi N, Barth JH, Balen AH. The use of metformin for women with PCOS undergoing IVF treatment. *Hum Reprod* 2006;**21**:1416–1425.

Tosca L, Uzbekova S, Chabrolle C, Dupont J. Possible role of 5'AMP-activated protein kinase in the metformin-mediated arrest of bovine oocytes at the germinal vesicle stage during in vitro maturation. *Biol Reprod* 2007;**77**:452–465.

Tront JS, Hoffman B, Liebermann DA. Gadd45a suppresses Ras-driven mammary tumorigenesis by activation of c-Jun NH2-terminal kinase and p38 stress signaling resulting in apoptosis and senescence. *Cancer Res* 2006;**66**:8448–8454.

Violette MI, Madan P, Watson AJ. Na+/K+-ATPase regulates tight junction function formation and function during mouse preimplantation development. *Dev Biol* 2006;**289**:406–419.

Wale PL, Gardner DK. The effects of chemical and physical factors on mammalian embryo culture and their importance for the practice of assisted human reproduction. *Hum Reprod Update* 2016;**22**:2–22.

Watson AJ, Kidder GM. Immunofluorescence assessment of the timing of appearance and cellular distribution of Na/K-ATPase during mouse embryogenesis. *Dev Biol* 1988;**126**:80–90.

Watson AJ, Pape C, Emanuel JR, Levenson R, Kidder GM. Expression of Na, K-ATPase alpha and beta subunit genes during preimplantation development of the mouse. *Dev Genetics* 1990;**11**:41–48.

Watson AJ, Natale DR, Barcroft LC. Molecular regulation of blastocyst formation. *Anim Reprod Sci* 2004;**82–83**:583–592.

Wilcock C, Bailey CJ. Accumulation of metformin by tissues in the normal and diabetic mouse. *Xenobiotica* 1994;**24**:49–57.

Xie Y, Wang F, Puscheck EE, Rappolee DA. Pipetting causes shear stress and elevation of phosphorylated stress-activated protein kinase/jun kinase in preimplantation embryos. *Mol Reprod Dev* 2007;**74**:1287–1294.

Xie Y, Awonuga A, Liu J, Rings E, Puscheck EE, Rappolee DA. Stress induces AMP-dependent loss of potency factors Id2 and cdx2 in embryos and stem cells. *Stem Cells Dev* 2013;**22**:1564–1575.

Yokoyama Y, Iguchi K, Usui S, Hirano K. AMP-activated protein kinase modulates the gene expression of aquaporin 9 via forkhead box a2. *Arch Biochem Biophys* 2011;**515**:80–88.

Zhan Q. Gadd45a, a p53- and BRCA1-regulated stress protein, in cellular response to DNA damage. *Mutat Res* 2005;**569**:133–143.

Zhang L, Li J, Young LH, Caplan MJ. AMP-activated protein kinase regulates the assembly of epithelial tight junctions. *Proc Natl Acad Sci USA* 2006;**103**:17272–17277.

Zheng B, Cantley LC. Regulation of epithelial tight junction assembly and disassembly by AMP-activated protein kinase. *Proc Natl Acad Sci USA* 2007;**104**:819–822.

Zhong W, Xie Y, Abdallah M, Awonuga AO, Slater JA, Sipahi L, Puscheck EE, Rappolee DA. Cellular stress causes reversible, PRKAA1/2- and proteasome-dependent ID2 protein loss in trophoblast stem cells. *Reproduction* 2010;**140**:921–930.

Zhou G, Myers R, Li Y, Chen Y, Shen X, Fenyk-Melody J, Wu M, Ventre J, Doebber T, Fujii N *et al*. Role of AMP-activated protein kinase in the mechanism of metformin action. *J Clin Invest* 2001;**1008**:1167–1174.